Int. J. Heat Mass Transfer. Vol. 31, No. 10, pp. 1993–1998, 1988
Printed in Great Britain

0017-9310/88 \$3.00+0.00

Prediction of boiling dryout heat flux for restricted annular crevice

M.-C. CHYU

Department of Mechanical Engineering, Texas Tech. University, Lubbock, TX 79409-4289, U.S.A.

(*Received* 22 *September* 1987 *and in final form* 26 *February* 1988)

Abstract—The phenomenon of boiling crisis in a horizontal narrow annular geometry is analyzed by considering a buoyancy-driven two-phase flow in a vertical crevice. Conservation laws are formulated and solved analytically. A two-phase friction factor is determined using published experimental data. The effect of crevice axial length is also considered for a variety of working fluids. The predicting method based on the present work applies in wide ranges of annulus width and crevice length for a variety of fluids with a remarkable improvement in accuracy over the existing predicting methods.

INTRODUCTION

BOILING in a restricted annular geometry is commonly found in the tube–baffle regions, as shown in Fig. 1, in a horizontal shell-and-tube heat exchanger with boiling in the shell side, such as the kettle reboiler and vapor generator used in the process and chemical industries. Because the restricted geometry retards fluid circulation, localized dryout occurs at a heat flux significantly lower than that of an open tube. This may lead to deposition of impurities and possible chemical attack of the tube surface.

In relation to this topic, nucleate boiling has been studied for a restricted horizontal plate [1–3], a vertical open-ended narrow annulus [4], vertical closed-bottomed narrow annuli [5], and vertical eccentric annuli [6–8]. Boiling and dryout phenomena on a horizontal boiling tube with fluid flow restricted by a concentric baffle were investigated by Jensen *et al.* [9], and Hung and Yao [10]. By using a modified Reynolds number based on the vapor flow within the annular space, a scaling factor taking into account the density change for different fluids, and two dimensionless geometric groups, Jensen *et al.* [9] proposed the following empirical correlation for the dryout heat flux for a restricted annular region:

$$\left[\frac{q''_{\mathrm{C}}L(D/\delta)}{2i_{\mathrm{fg}}\mu_{\mathrm{g}}(D/\delta+1)}\right]\left(\frac{D}{2\delta}\right)\left(\frac{\rho_{\mathrm{f}}-\rho_{\mathrm{g}}}{\rho_{\mathrm{g}}}\right)^{0.78} = 2.994\times10^{5}\left(\frac{\delta}{L}\right)^{-0.213}. \quad (1)$$

However, this correlation was found unsatisfactory compared with the experimental data by Hung and Yao [10] particularly when the crevice is long in the axial direction. As listed in Table 1, the error in the critical heat flux predicted by the correlation of Jensen *et al.* can be as great as 91%. Alternatively, Hung and Yao [10] proposed a semi-empirical analysis based on the balance between the buoyancy driving force and the viscous drag force on the two-phase crevice flow. Dryout was assumed to occur when the flow quality reaches 100% at the top of the tube. A two-phase friction factor dependent upon densities of liquid and vapor and Bond number was empirically determined. The result is the following equation of dryout heat flux:

$$q''_{\mathrm{C}} = 0.0090[Bo^{0.5}(D/L)^{1.5}] \times(1-\mathrm{e}^{-1.8Bo})i_{\mathrm{fg}}\rho_{\mathrm{f}}^{0.5}[\sigma g(\rho_{\mathrm{f}}-\rho_{\mathrm{g}})]^{1/4}. \quad (2)$$

This model demonstrated a more accurate prediction for long crevices than that by Jensen *et al.*, however, its accuracy deteriorates for short crevices. As shown in Table 1, the error of the predicted dryout heat flux using Hung and Yao's method can be as great as 172% compared with the short crevice experimental data reported by Jensen [11]. Unfortunately, neither Jensen *et al.*'s nor Hung and Yao's method seems to be generally applicable to wide ranges of variables with acceptable accuracy. Therefore, a better predicting method is needed.

The present work proposes a model of boiling dryout on a restricted horizontal tube by considering the buoyancy-driven two-phase flow in a vertical crevice. Conservation laws are formulated and solved analytically; a two-phase friction factor is then determined based on experimental data. The effect of crevice length is also considered for different working fluids. Generally, this method predicts dryout heat flux with a remarkable improvement in accuracy in wider ranges of variables compared with existing methods.

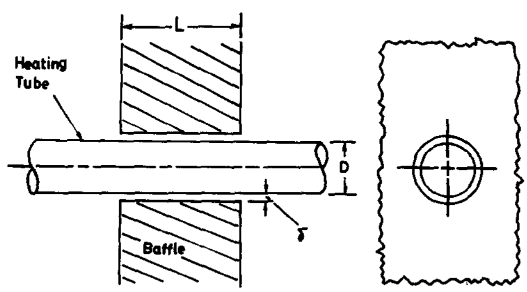

FIG. 1. The tube–baffle assembly.

NOMENCLATURE

Bo	Bond number, as defined in equation (19) [dimensionless]
D	diameter of the tube [m or mm]
f	friction factor [dimensionless]
F	force per unit width [N m^{-1}]
g	acceleration of gravity [m s^{-2}]
h	head loss [m]
i	specific enthalpy [J kg^{-1}]
K	factor defined in equation (20) [dimensionless]
l	length of channel defined in Fig. 2, $\pi D/2$ [m or mm]
L	length of the crevice, namely width of tube guide as defined in Fig. 1 [m or mm]
$\dot{m}$	mass flow rate [kg s^{-1}]
P	pressure [Pa]
$\dot{Q}$	total heat transfer rate [W]
q''	heat flux [W m^{-2}]
u	specific internal energy [J kg^{-1}]
V	mean velocity [m s^{-1}]
v	specific volume [m^3 kg^{-1}]
z	elevation [m].

Greek symbols

δ	annular clearance [m or mm]
ρ	density [kg m^{-3}]
σ	surface tension [N m^{-1}]
τ	shear stress at wall [N m^{-2}].

Subscripts

C	critical
f	liquid
fg	difference in property for saturated vapor and saturated liquid
fr	friction
g	vapor
w	weight
1,2	states defined in Fig. 2
1D	quantity based on one-dimensional consideration.

ANALYSIS AND CORRELATION

Two-phase friction factor

It was reported by Jensen *et al.* [9] that dryout always starts at the top-center point of the heating tube. Due to symmetry, the flow in the central section of the restricted annular geometry is scarcely influenced by the axial momentum of the liquid coming in through the annular opening, and the two-phase flow can be treated as one-dimensional, namely circumferential, in the central section where dryout occurs. Furthermore, because the gap size is generally very small compared with the tube diameter, the effect of curvature can be neglected. This leads to the consideration of a one-dimensional two-phase flow in a narrow vertical channel as shown in Fig. 2. The channel has a width the same as that of the annular gap, and a length of half of the tube circumference, $\pi D/2$. Only one of the walls is heated, while the other is insulated. This simulates a heating tube passing through an inactive baffle. Saturated liquid enters the channel at the bottom, and is vaporized by the heating

Table 1. Experimental and predicted data of critical heat flux (saturation, 1 atm)

Fluid	D (mm)	L (mm)	δ (mm)	Experimental q''_C (10^5 W m^{-2})	Percentage error in q''_C estimated using prediction method: Jensen *et al.* [9] equation (1)	Hung and Yao [10] equation (2)	Present work using equation (22)	Present work using equation (23)
Water [11]	12.75	12.29	0.076	1.4	−7.2	−42.4	0	−15.7
	12.75	12.29	0.16	2.6	−4.2	−4.4	3.8	−10.8
	12.75	12.29	0.254	5.20	36.2	−12.2	−23.1	−36.5
	12.75	12.29	0.356	4.35	−18.2	68.0	19.5	2.4
	12.75	12.29	0.508	8.01	14.8	48.2	−8.9	−25.0
	12.75	12.29	0.635	8.93	8.7	77.7	−2.2	−17.2
	12.75	12.29	1.02	10.4	−20.4	172.4	25.0	−4.7
	12.75	6.32	0.457	10.2	−7.7	−68.4	21.8	33.3
Water [10]	25.4	76.2	0.32	0.339	72.3	28.8	28.0	28.0
Freon-113 [10]	25.4	76.2	0.32	0.122	43.4	−22.5	0.1	0.1
	25.4	76.2	0.80	0.278	31.7	−5.7	−4.7	−4.7
	25.4	76.2	2.58	0.637	54.2	−1.1	14.8	14.8
	25.4	25.4	0.32	0.357	16.2	37.2	0	0.5
Acetone [10]	25.4	76.2	0.32	0.161	91.3	−29.6	15.7	15.7
	25.4	76.2	0.80	0.550	17.5	−35.8	−24.3	−24.3
	25.4	76.2	2.58	1.105	56.8	−9.2	2.8	2.8
	25.4	25.4	0.32	0.947	−22.7	−37.7	0	−24.1

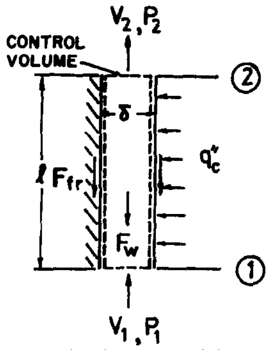

FIG. 2. Schematic of the dryout model treating the flow in an annular crevice as in a vertical channel.

wall while ascending due to buoyancy. Saturated vapor vents from the top at a much higher velocity because of the low vapor density compared with liquid.

With respect to the control volume including the space between the walls, conservation of momentum can be formulated as

$$(P_1-P_2)\delta-F_w-F_{fr} = (\rho_g V_2^2-\rho_f V_1^2)\delta. \quad (3)$$

Velocities V_1 and V_2 are the mean values of liquid at the inlet and vapor at the exit, respectively. The driving pressure force is due to the difference in hydrostatic pressure at the inlet and the exit; i.e.

$$P_1-P_2 = \rho_f g D. \quad (4)$$

The weight of the fluid in the control volume F_w is determined by assuming the average control volume quality to be 50%, and $v_g \gg v_f$. The 50% quality is based on the assumption that half of the liquid input is vaporized into vapor in the control volume all the time. Hence

$$F_w = 2\rho_g g l \delta. \quad (5)$$

The frictional force F_{fr} is due to the shear stress at the walls; thus

$$F_{fr} = 2\tau l. \quad (6)$$

By invoking the definition of the Darcy friction factor

$$f=\frac{8\tau}{\rho V^2} \quad (7)$$

and the Darcy–Weisbach equation

$$h_{fr} = f\frac{l}{2\delta}\frac{V^2}{2g} \quad (8)$$

the shear stress can be substituted for by a function of friction-head loss h_{fr}; the frictional force then becomes

$$F_{fr} = 2\rho_g g h_{fr}\delta. \quad (9)$$

Note $2\rho_g$ is taken as the average density of the control volume in this equation, which is based on the same assumption of 50% quality made for equation (5). By considering the conservation of mass, the flow momentum term on the right-hand side of equation (3) becomes

$$(\rho_g V_2^2-\rho_f V_1^2)\delta = \rho_g V_2^2[1-(\rho_g/\rho_f)]\delta$$
$$\cong \rho_g V_2^2\delta. \quad (10)$$

By substituting equations (4), (5), (9) and (10) into equation (3), the vapor velocity at the exit is determined as

$$V_2 = \{g[(\rho_f/\rho_g)D-2(l+h_{fr})]\}^{1/2}. \quad (11)$$

An alternative expression can be obtained by substituting h_{fr} in the last equation using equation (8) and solving for V_2; the channel length l can also be replaced by $\pi D/2$. Thus

$$V_2^2 = \frac{g(\rho_f/\rho_g-\pi)D}{1+(f\pi D/4\delta)}. \quad (12)$$

Now consider conservation of energy, namely the first law of thermodynamics, for the flow in the channel; the following equation is formulated:

$$\frac{\dot{Q}}{\dot{m}g}+\frac{P_1}{\rho_1 g}+\frac{V_1^2}{2g}+z_1 = \frac{P_2}{\rho_2 g}+\frac{V_2^2}{2g}$$
$$+z_2+\frac{u_2-u_1}{g}+h_{fr}. \quad (13)$$

The quantity $\dot{Q}$ is the heat rate to the control volume and the driving energy of the entire flow. Since the inlet pressure is greater than the exit pressure by $\rho_f g D$, the change in the static pressure head is

$$\frac{P_1}{\rho_1 g}-\frac{P_2}{\rho_2 g} = D-\frac{P_2 v_{fg}}{g}. \quad (14)$$

Noting that $z_1-z_2 = -D$, $u_2-u_1 = u_{fg}$, $i_{fg} = u_{fg}+Pv_{fg}$, $\dot{Q}/\dot{m} = (q''l)/\rho_g V_2^2\delta$, and V_1^2 is very small compared with V_2^2, one can obtain the following equation of dryout heat flux, namely the heat flux that vaporizes the entire flow of saturated liquid into saturated vapor when passing through the channel:

$$q''_{C,1D} = \frac{\rho_g V_2\delta}{l}\left(i_{fg}+\frac{V_2^2}{2}+h_{fr}g\right). \quad (15)$$

The subscript 1D designates the result based on a one-dimensional consideration. In reality, the last two terms in parentheses are usually numerically negligible compared with the first term, and the above equation reduces to

$$q''_{C,1D} = \frac{\rho_g V_2\delta i_{fg}}{l}. \quad (16)$$

Velocity V_2 can be substituted for using equation (11), thus

$$q''_{C,1D} = \frac{\rho_g\delta i_{fg}}{l}\{g[(\rho_f/\rho_g)D-2(l+h_{fr})]\}^{1/2} \quad (17)$$

where the length of the flow passage l is $\pi D/2$. The friction-head loss h_{fr} is defined by the Darcy–Weisbach equation (equation (8)). In this equation,

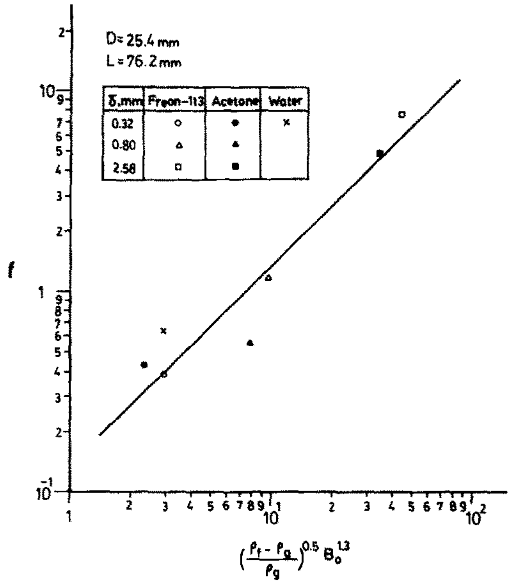

Fig. 3. Correlation of two-phase friction factor.

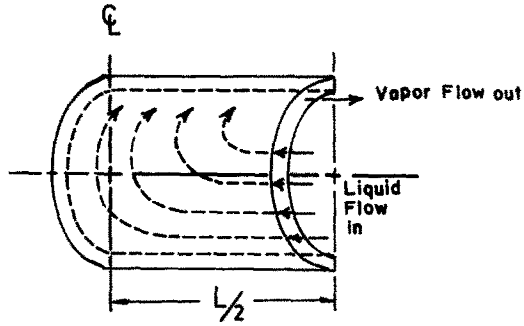

Fig. 4. Conceived flow pathlines in a quater of the annular crevice.

the two-phase friction factor f is a function of geometry and fluid properties to be determined based on experimental data.

Experimental dryout data for horizontal annular crevices of different dimensions using a variety of fluids have been reported by Jensen *et al.* [9], Jensen [11], and Hung and Yao [10]. Since the present analysis is basically for a one-dimensional flow, the data of axially long crevices are considered more suitable. This is based on the consideration that the two-phase flow in the central section of the restricted annular geometry, where dryout is most likely to occur, is less influenced by the motion of axial flow if the crevice is long. The critical heat flux data of a long crevice (76.2 mm in length, 25.4 mm in diameter) for Freon-13, acetone, and distilled water reported by Hung and Yao [10] are substituted into equation (17) to calculate the friction-head loss h_{fr}. The friction factor f is subsequently calculated using equation (8) with the exit vapor velocity V_2 given by equation (11) or equation (15). The f data so calculated are presented in Fig. 3. Hung and Yao [10] suggested that the two-phase friction factor is dependent upon ρ_f, ρ_g, as well as the Bond number to account for severe bubble deformation in a narrow crevice. The data are thus correlated by the following equation:

$$f = 0.13\left(\frac{\rho_f - \rho_g}{\rho_g}\right)^{0.5} Bo^{1.3} \tag{18}$$

where the Bond number is defined as

$$Bo = \delta\left[\frac{g}{\sigma}(\rho_f - \rho_g)\right]^{1/2}. \tag{19}$$

The above analysis assumes one-dimensional two-phase flow in the annular crevice. It can predict critical heat flux data for a long crevice with a satisfactory accuracy (within 28% for a 76.2 mm long crevice). It is noted that the length of the crevice did not participate as a factor in the analysis. However, both physical consideration and experimental data suggest that the critical heat flux depends upon the crevice length. This effect will be considered in the following section.

Effect of crevice length

The previous analysis is based on the assumption that the two-phase crevice flow is one-dimensional; i.e. the flow is upward and free from the influence of the axial momentum of the liquid coming in through the annular opening. This assumption is considered to be valid for the flow in the central section of an axially long annular crevice. However, in a relatively short crevice, there is an extra amount of flow in the axial direction due to the liquid coming in through the annular opening. It therefore takes a higher heat flux to vaporize the entire liquid flow, and the previous one-dimensional analysis tends to underestimate the critical heat flux.

Irrespective of the length of the crevice, the surrounding liquid can always feed into the crevice through the annular opening everywhere except near the top where vapor vents in the form of bubbles. Liquid which enters near the top of the annular opening would travel an axial distance shorter than that which enters near the bottom; this is because buoyancy forces the flow to move upward so that it reaches the top before having penetrated axially deep. Figure 4 illustrates the conceived flow pathlines in a quarter of the annular crevice. Near the center line of the geometry, the flow is considered to be basically one-dimensional. This is the premise that the analysis in the previous section relies on. However, for a short crevice, the effect of the liquid flow in the axial direction would be significant. In effect, this means an extra amount of liquid to be vaporized in addition to that considered in the one-dimensional model. This also means a higher heat flux is needed in order to vaporize the entire flow of liquid input. Therefore, the critical heat flux for a short crevice can be assumed to be related to that of a long crevice of the same gap width,

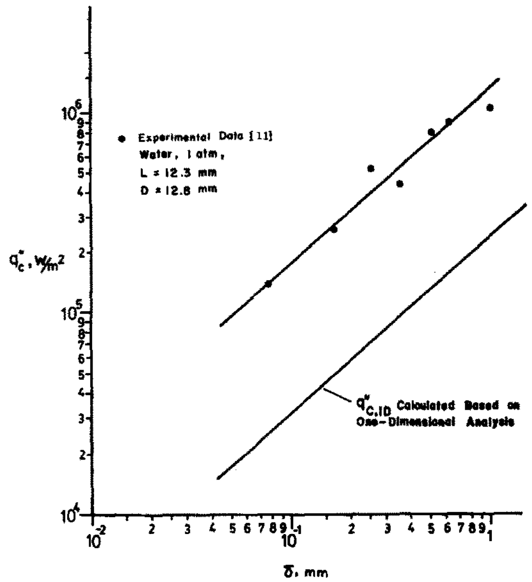

FIG. 5. Comparison of experimental critical heat flux data of a short crevice with calculations based on one-dimensional analysis.

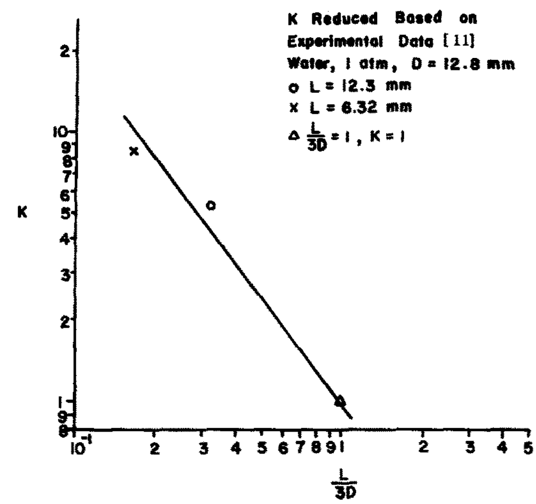

FIG. 6. Factor K of water vs non-dimensional crevice length.

tube diameter and fluid properties by the following simple equation:

$$q''_C = Kq''_{C,1D}. \tag{20}$$

This equation assumes that the critical heat flux of a short crevice is greater than that of a long crevice by a factor K. The factor K is a function of crevice length, diameter, and fluid properties.

In order to determine the factor K, experimental critical heat flux data for short annular crevices are compared with the data calculated based upon the one-dimensional analysis. This is exhibited in Fig. 5 where experimental data [11] of water boiling in a short crevice ($L = 12.3$ mm) of different gap widths are compared with calculated $q''_{C,1D}$. The data of $q''_{C,1D}$ are calculated by equation (16) while using equation (12) for V_2, equation (18) for factor f and equation (19) for the Bond number. The parallelism between the two data lines confirms the relation between the experimental data and the calculated $q''_{C,1D}$ as suggested by equation (20). The proportional factor K can thus be determined based on the plot. Figure 6 exhibits the K data so determined (denoted by an open circle) vs the ratio of non-dimensionalized crevice length L/D to that of a 76.2 mm long, 25.4 mm diameter crevice of which the non-dimensionalized crevice length is 76.2/25.4 = 3.00. This 76.2 mm long crevice is taken as a reference geometry because dryout data of this crevice were employed to develop the correlation for the friction factor f as given by equation (18) wherewith the $q''_{C,1D}$ data in Fig. 5 were calculated. By the same token, it is clear that K is unity at $L/(3D)$ equal to one, as shown in Fig. 6. Jensen [11] also reported data from an even shorter crevice ($L = 6.32$ mm). The K data marked by a cross in Fig. 6 was based on that data and its corresponding $q''_{C,1D}$. The factor K and the ratio of dimensionless crevice lengths thus can be correlated by the following equation based on Fig. 6:

$$K = \left(\frac{L}{3D}\right)^m. \tag{21}$$

A power index $m = -1.3$ is found suitable for water.

In addition to water, limited short crevice dryout data with Freon-113 and acetone are available [11]. The same procedure is followed to determine the K vs $L/(3D)$ relation. A relation similar to equation (21) applies to these fluids. The power index data of different fluids are

$$m = \begin{cases} -0.97 & \text{Freon-113} \\ -1.46 & \text{acetone} \\ -1.30 & \text{water.} \end{cases} \tag{22}$$

These m data can be roughly correlated as

$$m = -6.34\left(\frac{\mu_g}{\mu_f}\right)^{0.49}. \tag{23}$$

In this correlation, the power index m is taken to be a function of the viscosity ratio of the fluid because it is related to the rate of axial flow. However, this correlation is considered to be tentative because of insufficient data.

SUMMARY

In summary, the proposed prediction method based on the present analysis includes the following calculation steps:

(a) the Bond number defined by equation (19);
(b) the two-phase friction factor f given by equation (18);
(c) the velocity V_2 using equation (12);
(d) $q''_{C,1D}$ using equation (16);

(e) the factor K given by equation (21), and equation (22) or (23);

(f) the critical heat flux using equation (20).

The present method predicts the critical heat flux in restricted annular geometries with significantly better accuracy than existing predicting methods. As shown in Table 1, compared with experimental data available, the error of the present method is within 25% if the power index data regarding factor K for individual fluids as given in equation (22) are used, and 36% if a correlation given by equation (23) is used.

It is clear that this is not a complete analytical model. Also, this analysis is not suitable for the situation where there is a pressure difference across the baffle. The factors f and K in the present method are determined based on the published experimental data listed in Table 1. Additional data of different crevice dimensions using a larger variety of boiling fluids would be helpful in developing a prediction method for a wider range of application.

Acknowledgements—This material is based upon work supported by the National Science Foundation under Grant No. CBT-8504655. Advice from Professor S.-C. Yao at Carnegie-Mellon University and Professor M. K. Jensen at Rensselaer Polytechnic Institute, is gratefully acknowledged.

REFERENCES

1. Y. Katto and S. Yokoya, Experimental study of nucleate pool boiling in case of making interference-plate approach to the heating surface, *Proc. Third Int. Heat Transfer Conf.*, pp. 219–227 (1966).
2. Y. Katto and S. Yokoya, Principle mechanism of boiling crisis in pool boiling, *Int. J. Heat Mass Transfer* **11**, 993–1002 (1968).
3. Y. Katto, S. Yokoya and M. Ysunaka, Mechanism of boiling crisis and transition boiling in pool boiling, *Proc. Fourth Int. Heat Transfer Conf.*, Vol. 5, p. B3.2 (1970).
4. E. Ishibashi and K. Nishikawa, Saturated boiling heat transfer in narrow space, *Int. J. Heat Mass Transfer* **12**, 863–894 (1969).
5. S. C. Yao and Y. Chang, Pool boiling heat transfer in confined spaces, *Int. J. Heat Mass Transfer* **26**, 841–848 (1983).
6. B. S. Johnston, A. Sharon, Y. Kozawa and S. G. Bankoff, Boiling heat transfer in a narrow eccentric annulus, Part I. Dryout, *J. Engng Pwr* **105**, 742–747 (1983).
7. B. S. Johnston, A. Sharon and S. G. Bankoff, Boiling heat transfer in a narrow eccenric annulus, Part II. Heat transfer, *J. Engng Pwr* **105**, 748–754 (1983).
8. B. S. Johnston and S. G. Bankoff, Boiling heat transfer in a narrow eccentric annulus: Part III—A model of dry patch extent and temperature distribution, *J. Heat Transfer* **108**, 433–440 (1986).
9. M. K. Jensen, P. E. Cooper and A. E. Bergles, Boiling heat transfer and dryout in restricted annular geometries, Paper No. AIChE-14, pp. 205–214 (1976).
10. Y.-H. Hung and S.-C. Yao, Pool boiling heat transfer in narrow horizontal annular crevices, *J. Heat Transfer* **107**, 656–682 (1985).
11. M. K. Jensen, Boiling heat transfer and dryout in restricted geometries, Master of Science Thesis, Iowa State University, Ames, Iowa (1976).

PREDICTION DU FLUX THERMIQUE DE L'ASSECHEMENT PAR EBULLITION POUR UNE FISSURE ANNULAIRE ETROITE

Résumé—Le phénomène de l'ébullition critique dans une géométrie annulaire étroite est analysé en considérant un écoulement diphasique dans une crevasse verticale. Des lois de conservation sont formulées et résolues analytiquement. Un coefficient de frottement diphasique est déterminé en utilisant des données expérimentales déjà publiées. L'effet de la longueur axiale de la crevasse est considéré pour une variété de fluides. La méthode de prédiction basée sur le présent travail s'applique dans un large domaine de largeur d'anneau et de longueur de crevasse pour une variété de fluides avec une remarquable augmentation de la précision par rapport aux méthodes existantes.

BESTIMMUNG DER WÄRMESTROMDICHTE FÜR DEN DRYOUT IN RINGSPALTEN

Zusammenfassung—Es wird die Siedekrise in horizontalen engen Ringspalten untersucht unter Beachtung der auftriebsgetriebenen Zweiphasenströmung in einem senkrechten Spalt. Die Erhaltungsgleichungen werden formuliert und analytisch gelöst. Es wird ein Zweiphasen-Reibungsfaktor aus veröffentlichten experimentellen Daten bestimmt. Ebenso wird der Einfluß der axialen Länge des Spaltes für eine Vielzahl von Fluiden betrachtet. Das Berechnungsverfahren der vorliegenden Arbeit zeigt in einem weiten Bereich der Spaltweite und Spaltlänge für eine Vielzahl von Fluiden eine beträchtliche Verbesserung in der Genauigkeit gegenüber bestehenden Verfahren.

РАСЧЕТ ТЕПЛОВОГО ПОТОКА ПРИ КРИЗИСЕ КИПЕНИЯ В ОГРАНИЧЕННОЙ КОЛЬЦЕВОЙ ЩЕЛИ

Аннотация—Явление кризиса кипения в горизонтальном узком кольцевом канале анализируется на основании двухфазного свободноконвективного течения в вертикальной узкой щели. Сформулированы и решены аналитические уравнения сохранения. С помощью опубликованных экспериментальных данных определен коэффициент трения для двухфазного потока. Также рассмотрено влияние длины зазора для целого ряда рабочих жидкостей. Метод расчета, основанный на результатах данной работы, справедлив в широком диапазоне значений ширины и длины кольцевых зазоров для целого ряда жидкостей и дает более точные результаты, чем ранее использовавшиеся методы.